INASS

International Journal of
Intelligent Engineering & Systems

http://www.inass.org/

Performance Analysis of Tunable Band Pass Filter and VCO for Multiband RF Front End

J.Manjula*, S.Malarvizhi

ECE department, SRM University, Kattangulathur, Tamil Nadu -603203, India

* *Corresponding author's Email: jmanjulathiyagu@gmail.com*

Abstract: This paper presents a design and performance analysis of tunable RF front end circuits such as RF band pass filter and VCO for multiband applications. The tunable element is an active inductor, built by MOS transistors. It is attractive due to its tunable and larger inductance values. The RF band pass filter is realized using active inductor with suitable input and output buffer stages. The tuning of center frequency for multiband operation is achieved through the controllable current source of the active inductor. The tunable range of the band pass filter varies from 3.9 GHz to 12.3 GHz. The simulation results of band pass filter have minimum noise figure of 23 dB and has less power dissipation of 2.83mW. The simulated IIP3 is -9.6dBm for 1st and 3rd order frequency of 7.94 GHz and 7.93 GHz respectively. The VCO designed using active inductor has the tuning range of 0.384 GHz to 1.620 GHz with the phase noise of -139dBc/Hz at the offset of 1MHz. It consumes less power of 1.754mW with the figure of merit of 189dBc/Hz. The designed active inductor, RF band pass filter and VCO are simulated in 180nm CMOS process using Synopsys simulation tool.

Keywords: Active inductor; Input impedance; Phase noise; Multi band RF front end

1. Introduction

The design of multi-band RF front end has stimulated the development of compact and hardware sharing transceivers in RF systems. CMOS technology plays a vital role in the design of highly integrated, low power and low cost RF systems. The block diagram of a multi-band RF front end is shown in Fig.1. An analog RF band pass filter is an essential block of RF front end to select interested band in the received signal over entire spectrum. Low noise figure, low power consumption, tuning center frequencies and better linearity are some of the major challenges in the design of multiband RF band pass filter. Voltage controlled oscillator (VCO) is an important block of the RF front end which is used in frequency synthesizers to achieve absolute synchronization of local oscillator (LO) signals. The important specifications of VCO are center frequency, tuning range, power supply voltage, power consumption and phase noise. Most of the RF bandpass filters and VCO are implemented using on-chip spiral inductors [1]. But the spiral inductors cannot be realized for larger inductance values, high quality factor and smaller chip area [2]. On the other hand, active inductors can be realized for large inductance value with high resonance frequency, high quality factor, small chip area and wide range of tuning ability [3-6].

Active filters in GHz range have been designed in [7-8] and are not able to achieve the wide range of operating frequencies needed for multi standard RF systems. Widely tunable filters using varactors to change the operating frequencies have been designed in [9]. However, the varactors consume larger area and have less tuning range [10]. A fully integrated active LC band pass filter based on triple coupled spiral inductor topology has high power dissipation and less center

frequency tuning range [11]. A second-order active band pass filter using integrated inductors implemented in Si bipolar technology consumes high power dissipation of 68mW [12].

VCOs designed using active inductors are discussed in [13-16] have wide frequency tuning ranges and consume small amounts of power has shown an interest in the design of VCOs using active inductors. Furthermore, active inductor tuned VCOs are highly integrated and more cost effective than varactor tuned VCOs [17].

This task is to design a low power, low noise tunable RF band pass filter and VCO using active inductor for center frequency tuning. Section 2 briefly describes design and simulation results of active inductor, band pass filter and VCO.

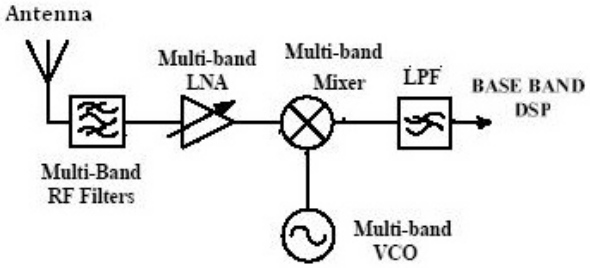

Figure 1 Block diagram of multi band RF front end

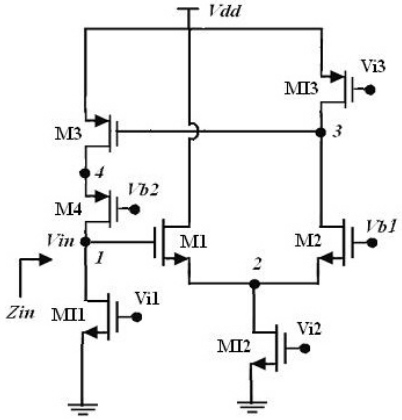

Figure 2 Circuit diagram of proposed single ended active inductor (with biasing arrangement) with the aspect ratios (W/L in μm) are M1(2.25 /0.18), M2 (2.25 /0.18), M3(4.5/0.18) & M4(4.5/0.18).

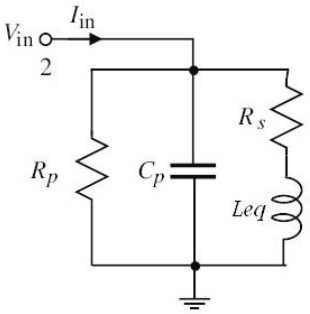

Figure 3 Passive equivalent circuit

2. Design and Simulation Results

2.1 Active inductor

A single ended active inductor is realized using gyrator-C topology [5] is an impedance inverter consisting of positive transconductor G_{m1} and negative transconductor G_{m2} connected back to back converts the port (parasitic) capacitances into an equivalent inductance. The proposed single ended active inductor with the aspect ratios in μm is shown in Fig. 2. It consists of differential pair M1 and M2 which represents the positive transconductor G_{m1} between the input (node 1) and the output (node 3). The cascode pair M3 and M4 represents the negative transconductor $-G_{m2}$ between the input (node 3) and the output (node 1). Thus the G_{m1} and $-G_{m2}$ forms the gyrator which converts the parasitic capacitance C_3 at node 3 to an equivalent inductance $L_{eq} = C_3/G_{m1}G_{m2}$. The passive equivalent circuit of the proposed single ended active inductor is shown in Fig.3.

The differential configuration of G_{m1} makes the proposed active inductor, less sensitive to noise and interference. The PMOS cascode structure of negative transconductor $-G_{m2}$, leads to possible negative resistance in series with the equivalent inductor to compensate the inductor loss. Thereby, it enhances the quality factor of the active inductor. Also, the cascode structure provides frequency range expansion by lowering the lower bound of the frequency range, thus increases the inductive bandwidth. The p-channel transistors are preferred for cascode structure as they have low noise and can be placed in separate n-wells, thus eliminating the non- linear body effect [4]. Thus, the combination of the differential configuration of G_{m1} and cascode configuration of $-G_{m2}$ offers higher inductive bandwidth, higher resonance frequency and less noise.

The equivalent input impedance Z_{in}, can be obtained from the small signal equivalent circuit of the active inductor where gm_{1-4} are the transconductances of M_{1-4}, C_{1-4}, g_{1-4} are the total parasitic capacitances and conductances at nodes 1-4 respectively.

$$Zin(s) = \frac{\frac{sg_4}{C_1} + \frac{g_3 g_4}{C_1 C_3}}{s^2 + s[\frac{g_1}{C_1} + \frac{g_1 g_3 C_2}{G C_1 C_3} + \frac{g_3}{C_3} - \frac{\omega^2 C_2}{G}]g_4 + \frac{gm_1 gm_2 gm_3 gm_4 + g_1 G g_3[gm_4 + g_4]}{G C_1 C_3}} \quad (1)$$

Where $G = gm_1 + gm_2 + g_2$.

The format of Z_{in} shows that it is equivalent to an RLC network, as shown in Fig. 3. Theesf term in the numerator indicates the equivalent inductance and the real term indicates series resistance.

From equation (1), L_{eq} and R_s can be written as,

$$Leq = \frac{g_4 G C_3}{gm_1 gm_2 gm_3 gm_4 + g_1 G g_3[gm_4 + g_4]} \quad (2)$$

$$Rs = \frac{G g_3 g_4}{gm_1 gm_2 gm_3 gm_4 + g_1 G g_3[gm_4 + g_4]} \quad (3)$$

The parallel capacitance $C_p = C_1$ and the parallel resistance $R_p = 1/g_2$.

The active inductor of Fig.2 with the given aspect ratios is simulated in 180nm CMOS process using Synopsys HSPICE simulator. The gate bias voltages are kept as Vb1=0.2V and Vb2=0.25V. The controllable current sources are I_1=90μA, I_2=80μA and I_3=100μA. The small signal parameters, gm_1 = 523μS, gm_2 = 724μS, gm_3 = 273μS, gm_4 = 873mS, g_1= 91μS, g_2= 84μS, g_3= 769μS, g_4= 109μS, C_1=1.87fF, C_2=1.53fF, C_3=4.03fF, C_4= 3.81fF and G= 1331μS are found from the operating points.

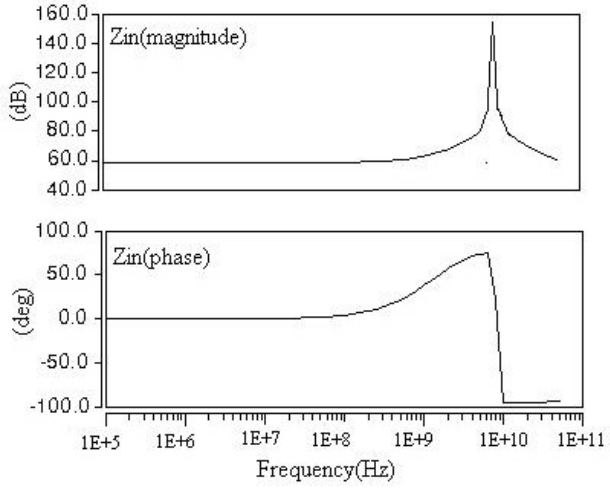

Figure 4 Simulated frequency response of input impedance

The simulated frequency response of Z_{in} is shown in Fig. 4. The magnitude of Z_{in} is nearly 150dB and the phase change is from +90° to -90°. The magnitude response shows that it has real term and imaginary term. It is constant at 58dB up to 1.5 MHz which is equivalent to the real term. The real term is the series resistance R_s, which is calculated to be 154Ω .

The response is increased from 1.5 MHz to 7.94 GHz which is equivalent to the imaginary term, the equivalent inductance L_{eq}. The value of inductance ranges from 125nH to 1530nH. Since it has less series resistance, the inductor loss is reduced. Fig. 5 shows the simulated inductance of the inductor.

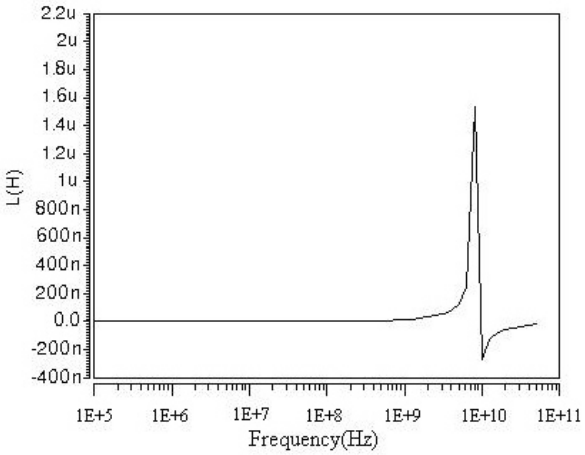

Figure 5 Simulated inductance

The quality factor Q_o at ω_0 is given as

$$Q_0 = \frac{\sqrt{\frac{gm_1 gm_2 gm_4 + g_1 G g_3[gm_4 + g_4]}{G C_1 C_3}}}{[\frac{g_1}{C_1} + \frac{g_1 g_3 C_2}{G C_1 C_3} + \frac{g_3}{C_3} - \frac{\omega^2 C_2}{G}]g_4} \quad (4)$$

From the real and imaginary values of the simulation results, the quality factor Q_o is calculated to be 497 at the frequency of f_o=7.94GHz. Fig. 6 shows the variation of Z_{in} for different values of controllable current source I_2. When I_2 is varied from 50μA to 120μA, the Z_{in} brings corresponding changes in R_s and L_{eq}. Therefore, the quality factor is tuned through the controllable current source I_2. The resonance frequency ω_0 is given as

$$\omega_0 = \sqrt{\frac{gm_1 gm_2 gm_4 + g_1 G g_3[gm_4 + g_4]}{G C_1 C_3}} \quad (5)$$

The center frequency f_o is tuned through the current source I3 of Fig. 2. Fig. 7 shows the tuning of

the active inductor for various centre frequencies. The controllable current source I_3 is varied from 30μA to 100μA for tuning the centre frequency of the active inductor. The designed active inductor has wide tuning range of 3.9GHz to 12.3 GHz. Table 1 shows the tuning of active inductor for various center frequencies for different values of controllable current source I_3.

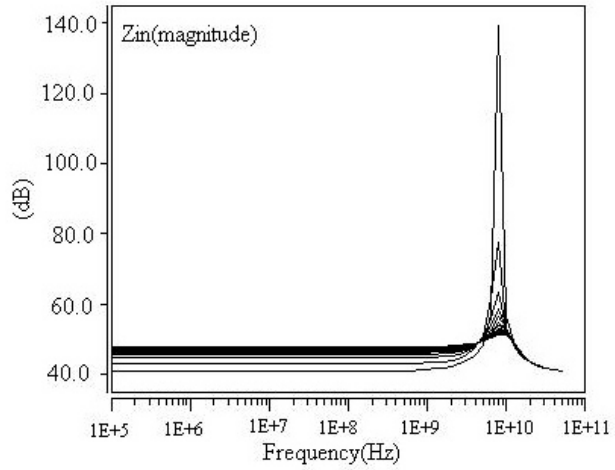

Figure 6 Quality factor tuning of the active inductor

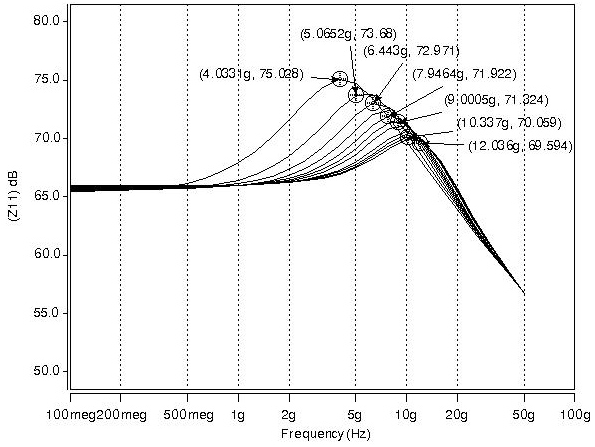

Figure 7 Center frequency tuning of the active inductor

The designed active inductor also features low power dissipation of 0.6mW. The noise output voltage varies from of 21nV/$\sqrt{Hz}$ to 7nV/$\sqrt{Hz}$ for the tuning range 3.9GHz to 12.3GHz. Fig. 8 shows the noise voltage (V^2/Hz) as a function of frequency. Fig. 9 shows the simulated noise figure of 3.5dB for the entire tuning range 3.9 GHz to 12.3 GHz. Fig. 10 shows IIP3 of -7.39dBm or 0.126Vpp, which has been simulated for 1st and 3rd order frequency of 7.94GHz and

Table 1 Center frequency tuning of active inductor

Controllable current spurce $I_3(\mu$ A)	Center frequency F_0(GHz)
72	3.99
67	4.99
64	6.3
61	7.94
55	9.9
42	12.3

7.93GHz respectively and has higher spurious free dynamic range of 118.7dB. The layout of the active inductor is shown in Fig. 11.

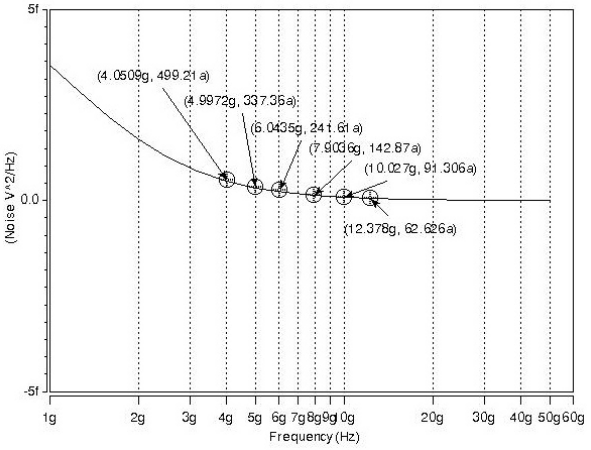

Figure 8 Noise voltage of the active inductor

2.2 Multi band RF band pass filter

The second order RF band pass filter of Fig. 12 is based on the active inductor topology. It consists of two resonators (M1, M2, M3, M4 and M5, M6, M7, M8) which are made up of single ended active inductors, coupled through the capacitance C [6]. Most of the band pass filter topologies used in thin film technology is of the coupled resonator type [18]. The advantage of coupled resonator filters is that they do not require a wide range of inductance values and are often realized using the same inductance for all resonators. The top coupled topology is one of the most commonly used. It is especially suitable to attenuate strong blocking signals in the cellular communications bands. However, in this type of filter the resonators operate in single ended mode. Min (W/L =1/0.18 in μm) is the common gate transistor, is used as the input buffer stage for input matching. A source follower stage Mout (W/L=1/0.18 in μm), is used as

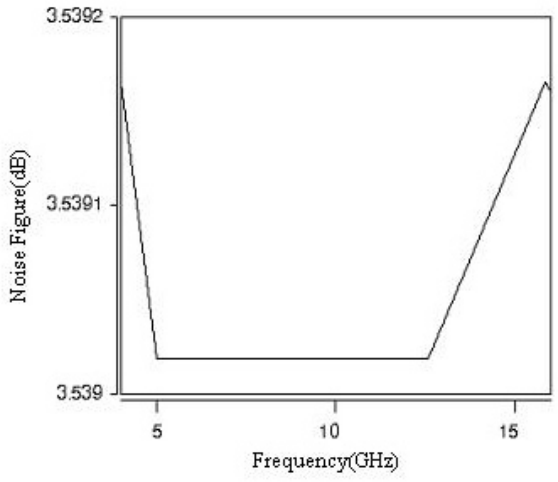

Figure 9 Noise figure of the active inductor

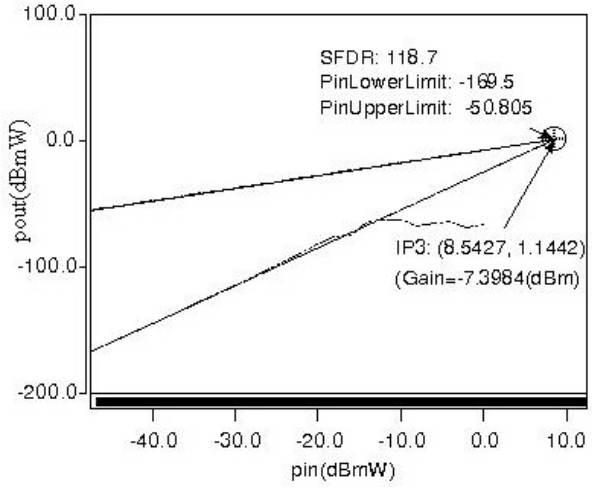

Figure 10 IIP3 of the active inductor

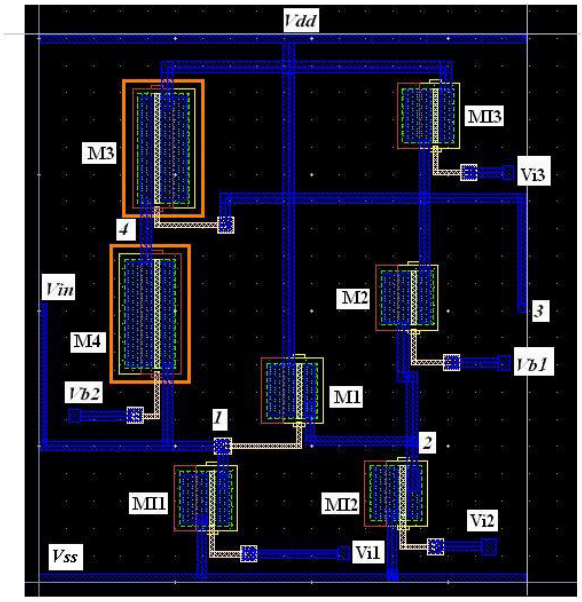

Figure 11 Layout of the active inductor

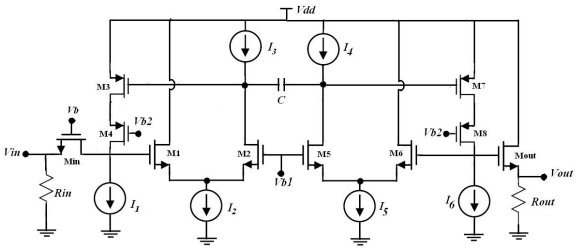

Figure 12 Circuit diagram of the RF band pass filter

an output buffer stage for output matching and to reduce the loading effect. Rin and Rout are the input and output resistances which are selected to be 1kΩ. The controllable current source I6 is used for tuning the center frequency of the band pass filter.

The frequency response of the band pass filter with 1KΩ at both ends (Rin at source and Rout at load) is shown in Fig. 13. It is simulated for center frequency of 7.94GHz with gain of 28dB and narrow bandwidth of 200MHz with less power consumption of 2.83mW.

With fixed Vb1 and Vb2, the center frequency can be tuned by varying controllable current source I_6 from 5μA to 110μA. The tuning range of the band pass filter is 3.99 GHz to 12.3 GHz. The tuning can be done through the single current source which adds advantage to this band pass filter. Table 2 lists the tuning of band pass filter for various center frequencies. Fig. 14 shows the simulation result of tuning of band pass filter for various center frequencies.

The simulated noise figure ranges from 27dB to 23dB for the entire tuning range 3.9 GHz to 12.3 GHz as shown in Fig. 15. The noise figure is 23dB for 7.94GHz. The IIP3 is -9.6012dBm or 0.1Vpp which has been simulated for 1st and 3rd order frequency of 7.94GHz and 7.93GHz respectively as in Fig. 16. The P_{1dB} compression point is -9.6dBm or 0.1Vpp from 50Ω source and higher spurious free dynamic range 94.101(dB) has been obtained.

2.3 Tunable VCO

The design of VCO is shown in Fig. 17. The topology of the VCO consists of cross coupled PMOS transistors to generate negative resistance and the resonant tank circuit [19]. The cross coupled PMOS transistors have smaller 1/f noise due to lower mobility comparing to NMOS transistors, and they have less hot carrier effect [20]. Thus PMOS VCO can achieve better phase noise performance and suppression of power supply noise than NMOS VCO. The resonant tank

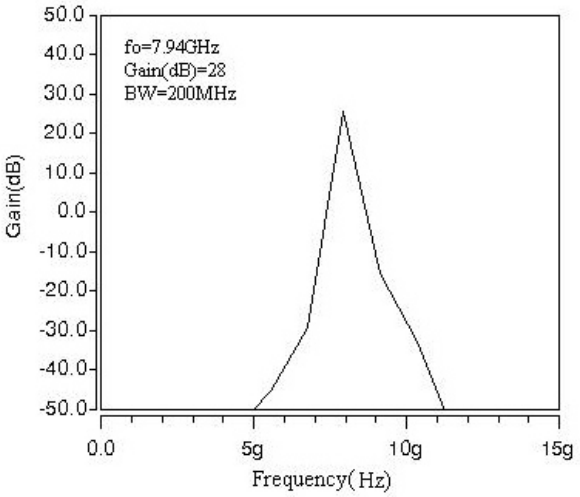

Figure 13 Frequency response of the band pass filter

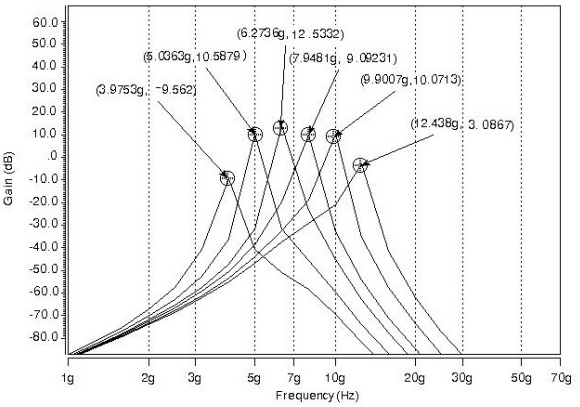

Figure 14 Tuning of band pass filter for various center frequencies

Table 2 Center frequency tuning of band pass filer

Controllable current spurce $I_6(\mu$ A)	Center frequency F_0(GHz)
5	3.99
10	4.99
19	6.3
35	7.94
60	9.9
110	12.3

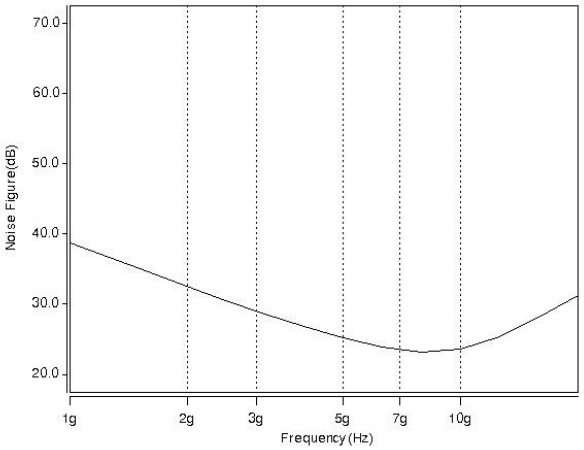

Figure 15 Noise figure of band pass filter

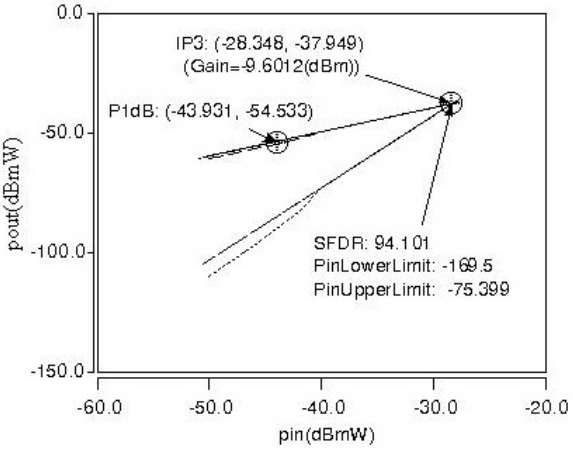

Figure 16 IIP3 of band pass filter

circuit is composed of a capacitor C and the active inductors L1 and L2. Active inductors are tunable and consume less power than spiral inductors. M3, M4, M5 and M6 forms the current reuse resistive feedback variable gain stage provides better output impedance matching. The oscillation frequency is given as equation (6) where L_{eq1} and L_{eq2} are the equivalent inductance of the active inductors L1 and L2 respectively. The equivalent inductances can be tuned through the controllable current source I2 of the active inductors which in turn vary the oscillation frequency.

Fig. 18 shows Vout+ and Vout- of VCO at f_{osc}=1.62GHz for I_2 =50μA. Fig. 19 shows the VCO output waveforms for the different frequencies with respect to the current source I_2 of the active inductors. The tuning range of the VCO is 0.384GHz to 1.62GHz. Fig. 20 shows the simulated phase noise of -139dBc/Hz at the offset of 1MHz. It consumes less power of 1.754mW as shown in Fig 21, with the figure of merit of 189dBc$\sqrt{Hz}$.

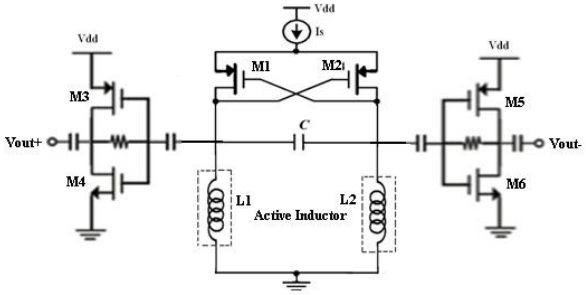

Figure 17 Circuit diagram of VCO

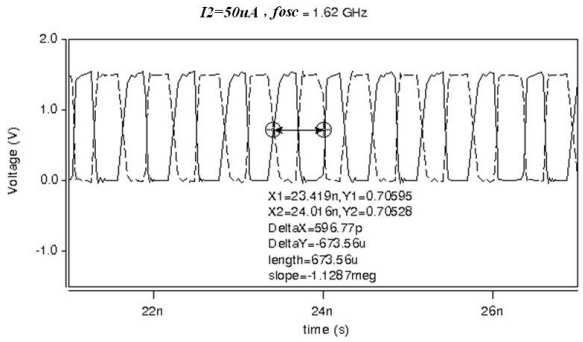

Figure 18 VCO output waveform for I_2=50μA

3. Performance Comparison

Table 3 compares the performances of band pass filter with reported works in the literatures [21, 22] of R-F band pass filters. The comparison results show that the band pass filter features wide range of center frequency tuning capability, less power dissipation and better linearity. Table 4 compares the performances of the VCO with the reported works in the literatures [23, 24, 25] of VCOs. The comparison results show that the designed VCO features better tuning range and low power consumption.

Table 3 Comparison of band pass filter performances

Parameter	Ref[21]	Ref[22]	This Work
Technology	90nm 1.2V	0.25μm 1.8V	0.18μm 1.8V
Filter order	2	2	2
ω_0(GHz)	3.46	1.6-2.45	3.99 -12.3
Power dissipation (mW)	1.4	8.6	2.83
NoiseFigure (dB)	5(at 3.46 GHz)	17(at 2.45GHz)	23(at 7.94GHz)
IIP3 (dBm)	-10.29	-2.1	-9.6

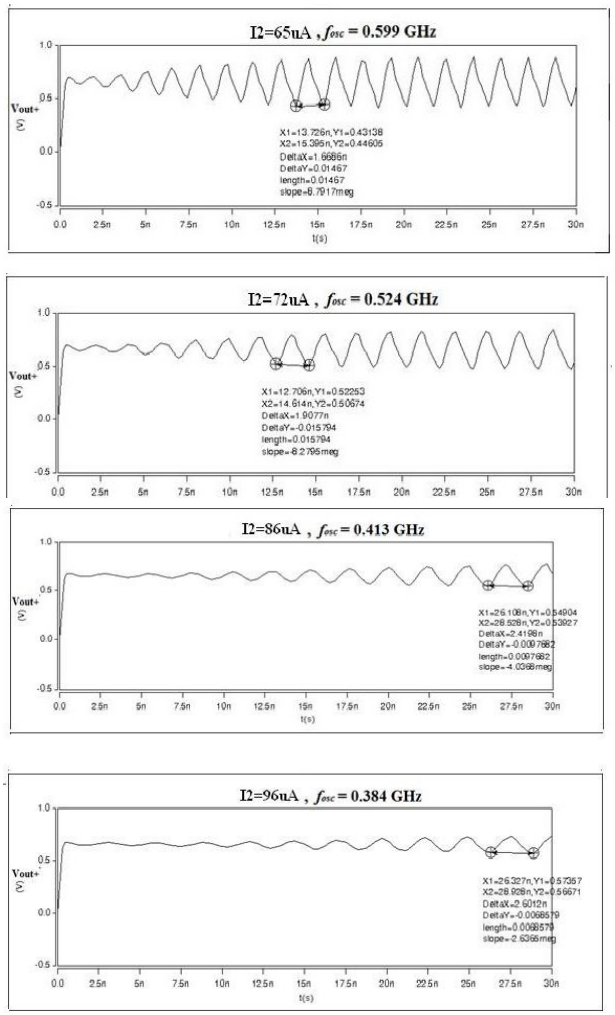

Figure 19 VCO output waveforms for different values of I_2.

4. Conclusions

The tunable RF band pass filter and VCO based on CMOS active inductor are simulated in 180nm CMOS process. The simulation results of active inductor show that the circuit has wide inductive bandwidth and high resonance frequencies. The simulation results of RF band pass filter prove that it has better tuning of center frequencies, less noise and lower power dissipation. The simulation result of VCO features lower power and better tuning range. The designed RF band pass filter and VCO are more suitable to design low power RF front end circuits.

References

[1] W. B. Kuh, F. W. Stephenson, and A. Elshabini-Riad,"A 200 MHz CMOS Q-enhanced LC band pass filter", *IEEE Journal of Solid-State Circuits*, Vol.31, No.8, pp.1112-1122, August 1996.

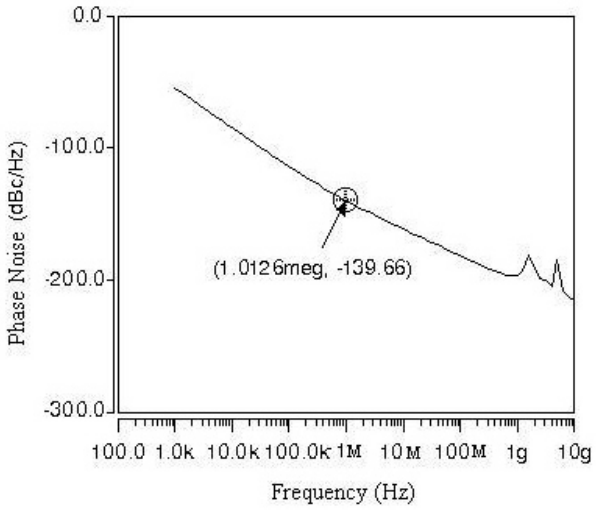

Figure 20 Simulated phase noise of VCO

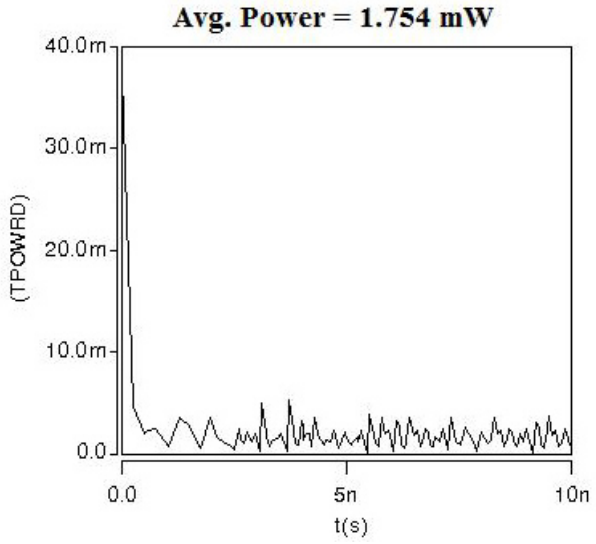

Figure 21 Average power consumption of VCO

Table 4 Comparison of VCO performances

Parameter	Ref[23]	Ref[24]	Ref[25]	This Work
Supply voltage(V)	2.6	1.8	1.8V	1.8
Technology (μm)	0.25	0.18	0.18	0.18
Frequency (GHz)	1	2/5.8	2.97 -4.45	0.384 -1.62
Phase Noise (dBc/Hz) at 1MHz	-130	-112/-107	-124.2	-139
Power (mW)	9	11.7/9.3	7	1.754

[2] A. Thanachyanont,"Low-voltage low-power high-Q CMOS RF band pass filter", *Electronics Letters*, Vol.38, No.13, pp.615-616, Jun 2002.

[3] H. Xiao and R. Schaumann,"A 5.4GHz high-Q tunable active-inductor band pass filter in standard digital CMOS technology", *Analog Integrated Circuits and Signal Processing*, Vol. 51, No. 1, pp. 1-9, 2007.

[4] A. Thanachayanont,"CMOS transistor-only active inductor for IF/RF applications", *IEEE International Conference on Industry Technology (ICITf02), Thailand*, Vol.2, pp. 1209-1212, Dec 2002.

[5] A. Thanachayanont and A.Payne,"VHF CMOS integrated active inductor", *Electronic Letters*, Vol.32, No.11, pp.999-1000, May 1996.

[6] M.M Reja, I.M. Filanovsky and K.Moez,"Wide Tunable CMOS Active Inductor", *Electronic Letters*, Vol. 44, No.25, pp. 1461-1463, December 2008.

[7] A. Thanachayanout and A.Payne,"CMOS floating Active Inductor and its Applications to Band Pass Filter and Oscillator Design", *IEE Proceedings on Circuits, Devices and Systems*, Vol. 147, No. 1, pp. 42-48, Feb 2000.

[8] F. Giannini, E.Limiti, G.Orengo and P.Sanzi,"High Q Gyrator based Monolithic Active Tunable Band stop Filter", *IEE Proceedings on Circuits, Devices and Systems*, Vol. 145, No. 4, pp. 243-246, August 1998.

[9] V. Aparin and P.Katzin,"Active GaAs MMIC Band Pass Filters with Automatic Tuning and Insertion Loss Control", *IEEE Journal of Solid State Circuits*, Vol. 30, No. 10, pp. 1068-1073, October 1995.

[10] W.M.Y. Wong, P.S.Hui, Z.Chen, K.Shen, J.Lau, P.C.H. Chan and P.Ko,"A Wide Tuning Range gated Varactor", *IEEE Journal of Solid State Circuits*, Vol. 35, No. 5, pp. 773-779, May 2000.

[11] S. Bantas, Y. Koutsoyannopoulos,"CMOS active-LC band pass filters with coupled inductor Q-enhancement and center frequency tuning", *IEEE Trans. Circuits and Systems-II: express briefs*, Vol. 51, pp.69-77 Feb. 2004.

[12] S.Pipilos, Y.P. Tsividis, J. Fenk, and Y. Papanaos,"A Si 1.8 GHz RLC filter with tunable center frequency and quality factor", *IEEE J. Solid-State Circuits*, Vol. 31, pp. 1517-1525, Oct. 1996.

[13] J. Laskar, R. Mukhopadhyay, and C.-H. Lee,"Active inductor-based oscillator:A promising candidate for low-cost low-power multi-standard signal generation", *in Proc. IEEE Radio Wireless Symp.*, Jan. 2007, pp.31-34.

[14] L.-H. Lu, H.-H. Hsieh, and Y.-T. Liao,"A wide tuning-range CMOS VCO with a differential tunable active inductor", *IEEE Trans. Microw. Theory Tech.*, vol. 54, no. 9, pp.3462-3468, Sep. 2006.

[15] R. Mukhopadhyay, Y. Park, P. Sen, N. Srirattana, J. Lee, C.-H. Lee, S. Nuttinck, A. Joseph, J. D. Cressler, and J. Laskar,"Reconfigurable RFICs in Si-based technologies for a compact intelligent RF

front-end", *IEEE Trans. Microw. Theory Tech.*, vol. 53, no. 1, pp.81-93, Jan. 2005.

[16] Y. Wu, M. Ismail, and H. Olsson,"CMOS VHF/RF CCO based on active inductors", *Electron. Lett.*, vol. 37, no. 8, pp.472-473, Apr. 2001.

[17] Ulrich L. Rohde, Ajay K.Poddar,"Tunable Active Inductor Offers Integrable And Cost-Effective Alternatives of Varactor Tuned VCOs", *IEEE International Frequency Control Symposium*, pp. 962-967, April 2009.

[18] Robert C Frye, Kai Liu, Guruprasad Badakere, Yaojian Lin,"A Hybrid Coupled - Resonator Band pass Filter Topology Implemented on Lossy Semiconductor Substrates", *IEEE/MTT-S International Microwave Symposium*, pp. 1757-1760, June 2007.

[19] Shirin Bahramirad, Jad G. Atallah, Steffen Albrecht,"A Low Phase Noise VCO for Multi Band Wireless Transceivers", *International Conference on Design & Technology of Integrated Systems in Nanoscale era*, pp. 148 -153, Sep. 2007.

[20] J. Y. Chen,"CMOS Devices and Technology for VLSI", *Englewood Cliffs, NJ: Prentice Hall*, Chapter 5, 1990.

[21] Santhosh Vema Krishnamurthy, Kamal El-Sankary, and Ezz El-Masry,"Noise-cancelling CMOS Active Inductor and Its Application in RF Band-Pass Filter Design", *International Journal of Microwave Science and Technology*, Vol. 2010, Article ID 980957, pp. 1 - 8, 2010.

[22] S. Bantas, Y. Koutsoyannopoulos,"CMOS active-LC band pass filters with coupled inductor Q-enhancement and center frequency tuning", *IEEE Trans. Circuits and Systems-II: express briefs*, Vol. 51, pp.69-77, Feb. 2004.

[23] Z. Tang, J. He, H. Min,"A Low Phase Noise 1-GHz LC VCO Differentially Tuned by Switched Step Capacitors", *IEEE Asian Solid State Circuits Conference*, 2005.

[24] M. Yeh, W. Liou, T. H. Chen, Y. C. Lin, J. Ho,"A Low Power 2/5.8 GHz CMOS LC VCO for Multi band Wireless Communication Applications", *International Conference on Communication, Circuits and Systems*, 2006.

[25] B. Q. Diep, C. S. Park,"All PMOS Wideband VCO for Multi band Multi Standard Radios", *The 9th International Conference on Advanced Communication Technology*, 2007.